5D.5   SIMULATION OF EL NINO-SOUTHERN OSCILLATION (ENSO) USING A HYBRID COORDINATE OCEAN MODEL (HYCOM)

Yanyun Liu, Lian Xie

North Carolina State University, Marine, Earth and Atmospheric Sciences, Raleigh, NC

John M. Morrison

University of North Carolina Wilmington, Department of Physics & Physical Oceanography

Wilmington, NC

1. INTRODUCTION

El Niño and Southern Oscillation (ENSO) is an atmosphere-ocean coupled phenomenon that exhibits interannual variability in tropical Pacific Ocean and plays an important role in modulating the interannual variability of regional climate globally. El Niño is defined by the appearance and persistence, for 6-18 month, of anomalously warm water in the coastal and equatorial ocean off Peru and Ecuador (Trenberth, 1997) and is a perturbation of the coupled ocean-atmosphere system. It is dynamically linked to the Southern Oscillation, a see-saw in surface atmospheric pressure between the Australian–East Asian region and the eastern tropical Pacific. Bjerkness (1969) first hypothesized that a positive ocean-atmosphere feedback involved the Walker circulation is responsible for the SST warming observed in the equatorial eastern and central Pacific. An initial positive sea surface temperature (SST) anomaly in the equatorial eastern Pacific reduces the east-west SST gradient and hence the strength of the Walker circulation (Gill, 1980; Lindzen and Nigam, 1987), resulting in weaker trade winds around the equator. A decrease of the equatorial easterlies weakens the equatorial upwelling, thereby the eastern equatorial Pacific becomes warmer and supplies heat also to the atmosphere above it. The weaker trade winds in turn drive the ocean circulation changes that further reinforce SST anomaly. This positive ocean-atmosphere feedback leads to the occurrence of El Niño.

* *Corresponding author address:* Yanyun Liu, North Carolina State Univ., Dept. of Marine, Earth & Atmospheric Sciences, Raleigh, NC 27695-8208; e-mail: yliu10@ncsu.edu.

In this study, we will simulate the ENSO events using the HYCOM with daily atmospheric forcing derived from the NCEP/NCAR reanalysis dataset.

2. MODEL CONFIGURATION AND NUMERICAL EXPERIMENTS

ENSO simulations were carried out using HYCOM with a grid size of 1.44° x 0.72° in zonal and meridional direction, respectively. The experiment domain covers the entire global ocean and has a vertical resolution defined by 26 layers that stretch or shrink vertically as a function of total depth according to the hybrid coordinate frame. The model was driven by daily surface wind stress, surface air temperature, surface atmospheric specific humidity, net shortwave radiation, net long-wave radiation and precipitation fields obtained from NCEP/NCAR reanalysis dataset for the period of 1949-2006 (Kistler, et al, 2001). The model was initialized with temperature and salinity from the Levitus monthly climatology (Levitus et al., 1994) and ran for 58 years. The latent and sensible heat fluxes were calculated during model runs using the model sea surface temperature and the bulk formulation (Cayan 1992). The KPP vertical mixing model of Large et al (1994) was also used and the bathymetry was from ETOPO2, and is interpolated on the model grids. The model was run for 58 years from 1949 to 2006.

3. PRELIMINARY RESULTS ABOUT ENSO SIMULATION USING HYCOM

ENSO variability from 1949 to 2006 was simulated using HYCOM using NCEP NCAR reanalysis atmospheric forcing. The area-averaged SST anomalies in the Nino3.4 region (5° S-5° N, 150° W-90° W) are often used to

index ENSO variability (Trenberth, 1997). Fig 1 shows the observed (blue) (don't use color, use line pattern instead) and HYCOM simulated (red) SST anomalies in Niño3.4 region from 1949 to 2006. The correlation coefficient between the simulated SSTA and observed SSTA is 0.721. The power spectrum of the SST anomalies (Fig 2) showed that the main ENSO period in the model is approximately from 3 to 7 years, similar to the observed main period. The peak amplitude of the power spectrum is comparable in the model and observations. This result indicates that the HYCOM can generally simulate major El Niño events especially the strong 1997-98 events.

However, the simulated SST anomalies (SSTA) in Niño3.4 region have an anomalous rising trend compared with the observed SSTA (see Fig 1). If we remove the trend from the SST anomalies series, the simulated SSTA is closer to the observations (see Fig 3). The correlation coefficient between the simulated SSTA and observed SSTA increases to 0.836. To extract the main signal with a period from 2-7 year, the SST anomalies in Niño3.4 region are band-pass filtered using a wavelet filter. Fig 4 shows the band-pass filtered observed (red, dashed) and HYCOM simulated SST anomalies (blue, solid) (again, don't use color) in Nino3.4 region from 1950 to 2006. The correlation coefficient between the simulated SSTA and observed SSTA increases to 0.913, which shows a near-perfect match between the model data and the observations at the interannual band. This suggests that even with the presence of erroneous trends in the simulated data, the model was able to accurately simulate the internnual variability in the tropical ocean.

3.1 DIAGNOSTIC STUDY OF ENSO SIMULATION

Diagnostic analysis of the ENSO simulations by HYCOM was carried out to try to understand the reasons for the simulated trend in the SSTA. In order to study the reason for this trend, we need to identify the factors which affect the sea surface temperature. The sea surface temperature can be influenced by horizontal advection, radiation flux, sensible and latent heat flux and entrainment/detrainment process. In HYCOM, the temperature governing equation in isopycnic coordinate is

$$\frac{\partial}{\partial t}(T\Delta p) + \underbrace{\nabla \cdot (\vec{u}T\Delta p)}_{advec} +$$

$$\underbrace{\left(\dot{s}\frac{\partial p}{\partial s}T\right)_{bot} - \left(\dot{s}\frac{\partial p}{\partial s}T\right)_{top}}_{dia-diff}$$

$$= \underbrace{\nabla \cdot (\upsilon\Delta p\Delta T)}_{iso-diff} + H_T$$

where Δp is the thickness of the layer with temperature T; γ is the eddy viscosity/diffusion coefficient and H_T is the radiative exchanges.

The expression $\left(\dot{s}\frac{\partial p}{\partial s}\right)$ is the vertical mass flux. The first term on left hand side (LHS) is the change of temperature in the mixed layer; the second term on the LHS is the horizontal advection term; the third is diapycnic diffusion term. On the right hand side, the first term is the isopycnic diffusion and the second term H_T the radiative term. The advection term is mainly determined by wind stress. Entrainment/Detrainment processes depend on both wind stress and buoy fluxes which are affected by sensible and latent heat fluxes and radiation.

In this study, HYCOM is driven by daily surface wind stress, surface air temperature, surface atmospheric specific humidity, net shortwave radiation, net longwave radiation and precipitation fields. The latent and sensible heat fluxes can be calculated during model runs using the model sea surface temperature and the bulk formulation. There are two choices for bulk parameterization schemes of surface fluxes due to different latent and sensible heat exchange coefficients in HYCOM. The first is the standard constant bulk coefficients. The second is the complex parameterization algorithm of Kara *et al.* (2000) for evaporation and air-sea heat fluxes has been included in HYCOM. The main difference of the two choices is due to the different parameterization of latent and sensible heat exchange coefficients. For the first choice, the exchange coefficients are constant and for the second, they are related to wind speed and air-sea temperature difference. In addition, the wind stress also has a great effect on the change of temperature via mechanical energy transfer.

The effect of ocean-atmosphere exchanges

(bulk formula) on the mixed layer is summed as follows:

$$B = R + H + \xi$$

where R is the net radiative exchanges, H is sensible heat flux and ξ is latent heat flux.

The sensible heat flux

$$H = C_{Pair} E_x (T_s - T_a) ;$$

where E_x is an exchange coefficient such that $E_x = \rho_a C_T W$, ρ_a means Mass/volume of the air; C_T is heat transfer coefficient; C_{Pair} is specific heat of the air; T_s is sea surface temperature; T_a is temperature in the atmosphere boundary layer; W is wind velocity.

The latent heat flux

$$\xi = E_x L (H_u - E_v) .$$

Where L is latent heat of vaporization; H_u is specific humidity; E_v is evaporation.

A possible reason for the rising trend of SST anomaly in Nino3.4 region may come from the surface forcing. Fig 5 showed the shortwave radiation and net radiation flux anomaly in Nino3.4 region from 1950 to 2006 from NCEP/NCAR dataset. The radiation heat fluxes also showed a rising trend. Fig 6 depicted the observed and simulated latent heat flux anomaly and sensible heat flux anomaly in Nino3.4 region from 1950 to 2006. Simulated results showed that the latent heat flux can been generally simulated by HYCOM, while the sensible heat flux, which also has a rising trend, has a large difference with the observed sensible flux. The reasons for this phenomenon may be associated with the rising trend of the simulated SST anomaly. The net heat flux also has a rising trend, similar to the shortwave heat flux. Fig 7 shows the HYCOM simulated SST anomalies in Nino3.4 region from 1950 to 2006 using the classic bulk formula method and Kara,2000). The SST simulations haven't a big difference in these three schemes. So there is a hypothesis that the rising trend of SST anomaly came from the surface forcing. To confirm this hypothesis, we compared the surface forcing from ECMWF to that from NCEP. Fig 8 depicts the radiation heat flux anomaly, solar radiation flux anomaly and thermal radiation flux anomaly in Nino3.4 region from NCEP and ECMWF dataset. There is a significant difference between the radiation heat flux in the NCEP/NCAR data and the

ECMWF data. The latter does not show the same rising trend in radiation fluxes as seen in the NCEP data. The effect of this trend in radiation flux in the simulated SST will be examined.

Another possible reason for the unrealistic rising trend produced in the model wasdue to weak model mixing than to trends in the surface forcing. This is a work in progress.

4. SUMMARIES

El Nino and Southern Oscillation is an atmosphere-ocean coupled phenomenon that exhibits interannual variability in tropical Pacific Ocean and plays an important role in modulating the interannual variability of regional climate globally. In this study, the ENSO events are simulated using the Hybrid Coordinate Ocean Model (HYCOM) with daily atmospheric forcing derived from the NCEP/NCAR reanalysis dataset for the period of 1949-2006. The result indicates that with prescribed atmospheric forcing, the HYCOM model can accurately simulate the major characteristics of ENSO events. The correlation coefficient between the simulated Sea Surface Temperature (SST) anomalies and observed SST anomalies in the Niño3.4 region is 0.73. However, the simulated SST anomalies (SSTA) have an anomalous rising trend compared with the observed SSTA. SST can be influenced by horizontal advection, radiation flux, sensible and latent heat flux and entrainment/detrainment process. Two choices of bulk parameterization schemes of surface fluxes due to different latent and sensible heat exchange coefficients are used in HYCOM. Sensitivity analysis shows the unrealistic rising trend produced by the model was more due to weak model mixing than to trends in the surface forcing. However, extracting the interannual band of the simulated tropical Pacific SST from the model data shows a near-perfect match between the model data and the observations at the interannual band. This suggests that even with the presence of erroneous trends in the simulated data, the model was able to accurately simulate the internnual variability in the tropical Pacific Ocean.

5. ACKNOWLEDGMENTS

6. REFERENCES

Bjerkness, J. 1969: Atmospheric teleconnections from the equatorial Pacific. Monthly Weather Review, 97, 163-172.

Bleck, R., 2002. An oceanic general circulation model framed in hybrid isopycnic-Cartesian coordinates. Ocean Modeling, 4, 55-88.

Cayan, D. R., 1992: Latent and sensible heat flux anomalies over the northern oceans: Driving the sea surface temperature. *J. Phys. Oceanogr.*, **22,** 859-881.
CD-ROM and Documentation. Bull. Amer. Meteor. Soc., 82, 247-268.

Levitus, S., Boyer, T., 1994. World Ocean Atlas 1994, Volume 4: Temperature. NOAA Atlas NESDIS 4. US Dept. of Commerce, Washington, DC.

Lindzen, R.S., and S. Nigam, 1987: On the role of sea surface temperature gradients in forcing

Chavez, F.P., Strutton, P.G., Friederich, G.E., Feely, R.A., Feldman, G.C., Foley, D.G., McPhaden, M.J., 1999. Biological and chemical response of the equatorial pacific ocean to the 1997–1998 El Niño. Science 286, 2126–2131.

Gill, A. E. 1980: Some simple solutions for heat-induced tropical circulation. *Quarterly Journal of Royal Meteorological Society*, 106, 447-462.

Kara A.B., P.A. Rochford and H.E. Hurlburt, An optimal definition for ocean mixed layer depth, *J. Geophys. Res.* **105** (2000), pp. 16,803–16,821.

Kistler, R., E. Kalnay, W. Collins, S. Saha, G. White, J. Woollen, M. Chelliah, W. Ebisuzaki, M. Kanamitsu, V. Kousky, H. van den Dool, R. Jenne, and M. Fiorino, 2001: The NCEP-NCAR 50-Year Reanalysis: Monthly Means

low level winds and conver-gence in the tropics. *J. Atmos. Sci., 44*, 2440-2458.

Trenberth, K.E., Hoar, T.J., 1997. El Niño and climate change. Geophysical Research Letters 24, 3057–3060.

Trenberth, K.E., 1997. The Definition of El Niño. Bulletin American Meteorological Society 78, 2771–2778.
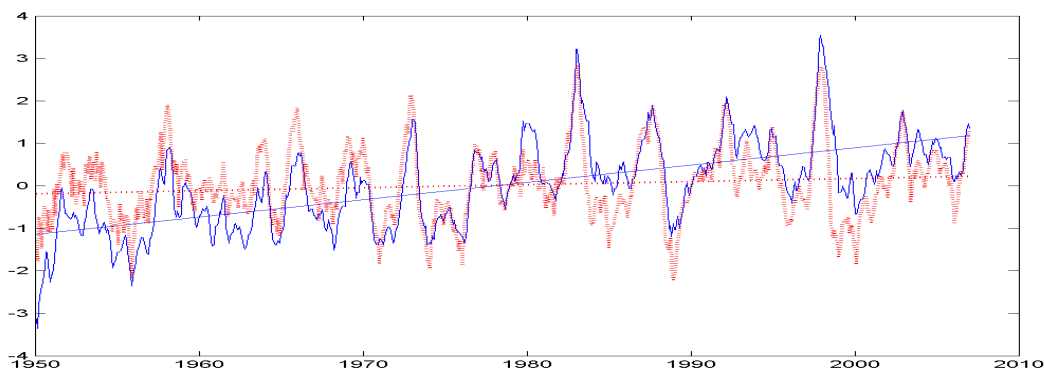
Fig. 1: The observed (red, dashed) and HYCOM simulated SST anomalies (blue, solid) in Nino3.4 region from 1950 to 2006.
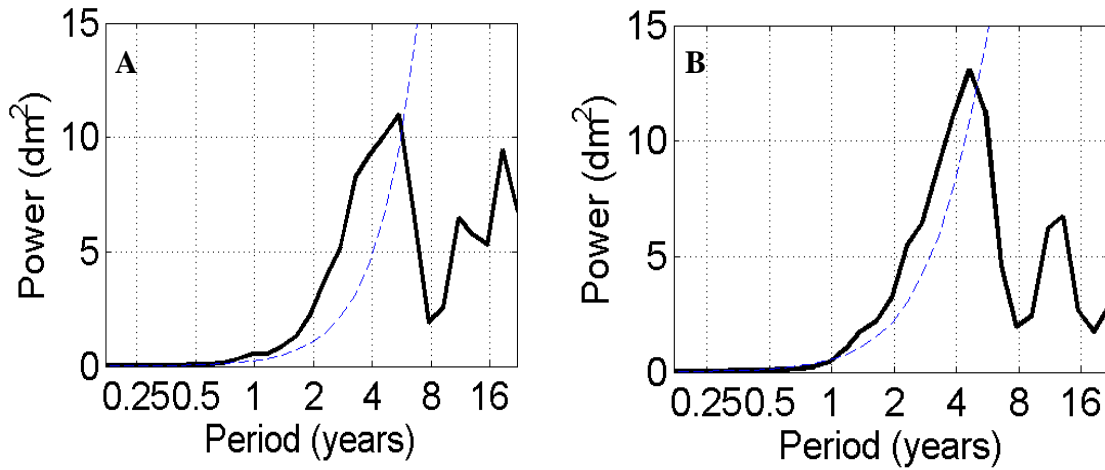
Fig. 2: The power spectrum of the SST anomalies in the Niño3 region during 1950- 2006: a) Model simulation; b) Observation.
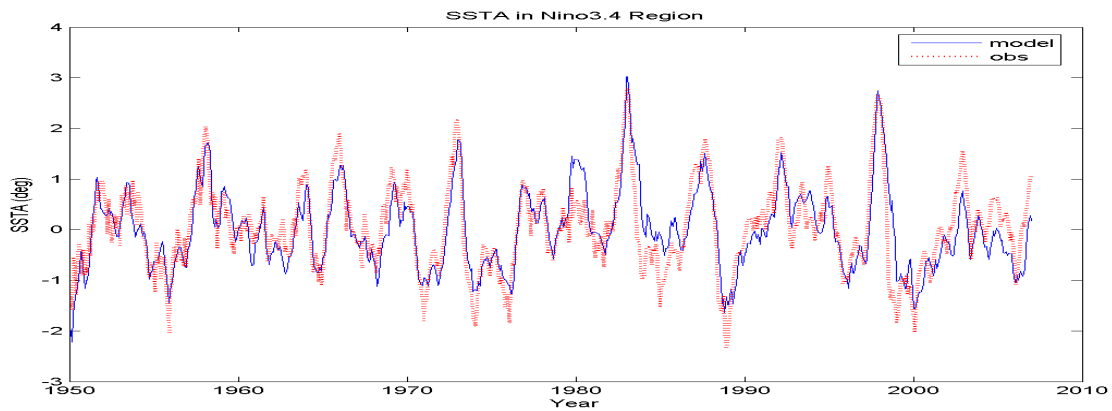
Fig. 3: The observed (red, dashed) and HYCOM simulated SST anomalies (blue, solid) in Nino3.4 region from 1950 to 2006 after subtracting the trend.
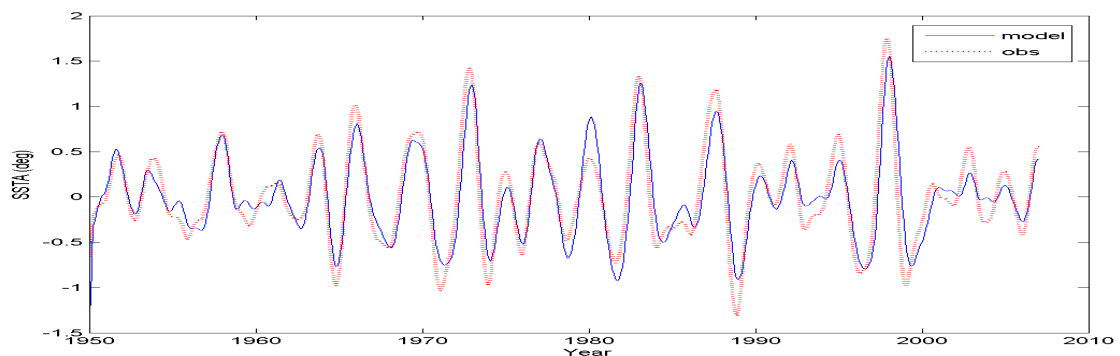
Fig. 4: The bandpass filtered observed (red, dashed) and HYCOM simulated SST anomalies (blue, solid) in Nino3.4 region from 1950 to 2006.
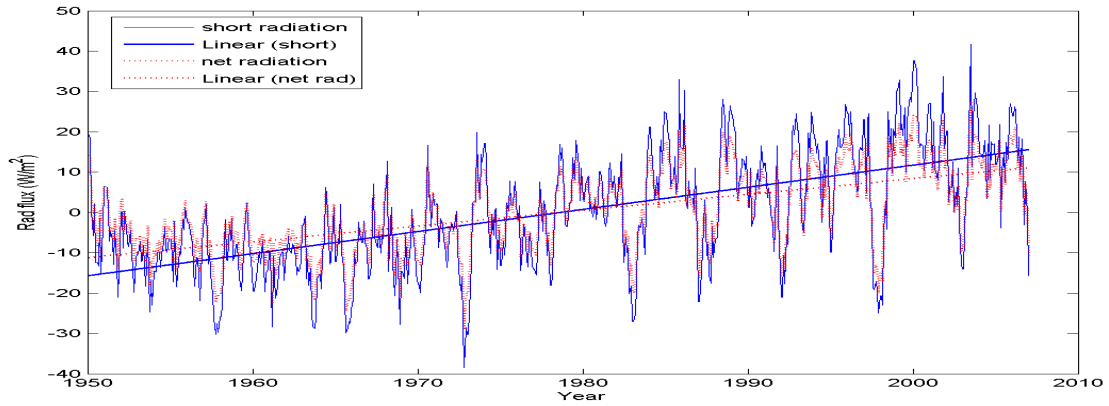
Fig. 5: The shortwave radiation anomaly (blue, solid) and net radiation flux anomaly (red, dashed) in Nino3.4 region from 1950 to 2006 from NCEP dataset.
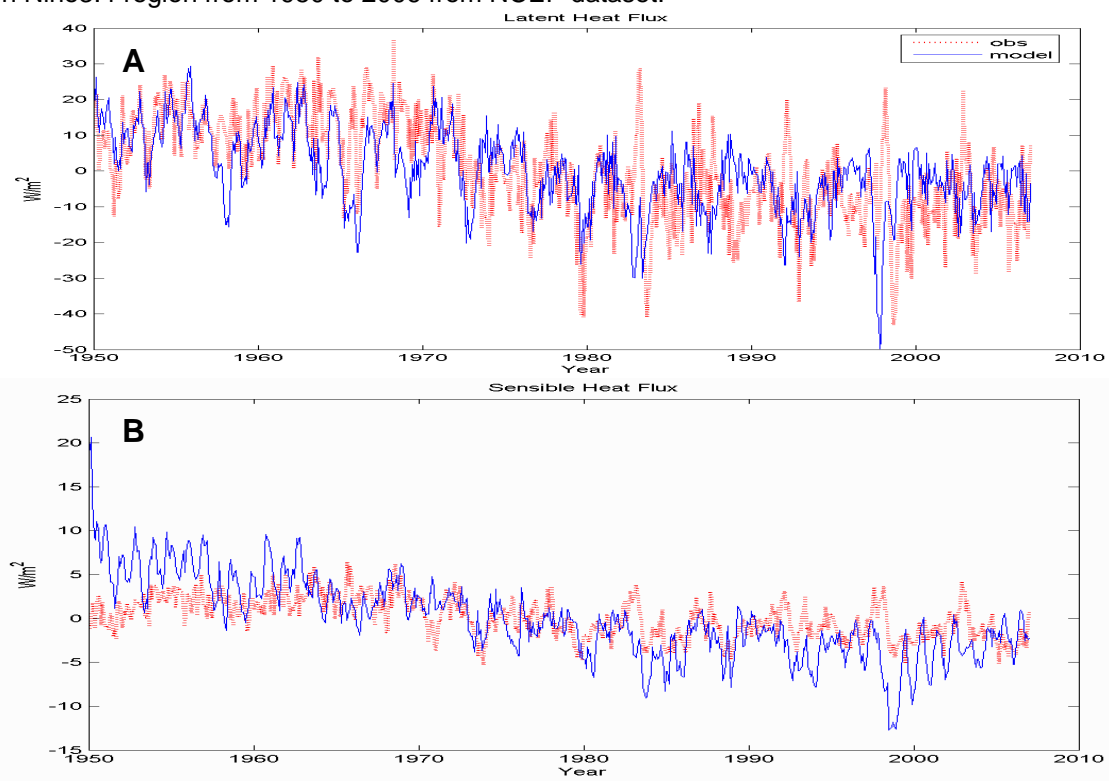
Fig. 6: The observed (red, dashed) and simulated (blue, solid) a) Latent heat flux anomaly and b) Sensible heat flux anomaly in Nino3.4 region from 1950 to 2006.
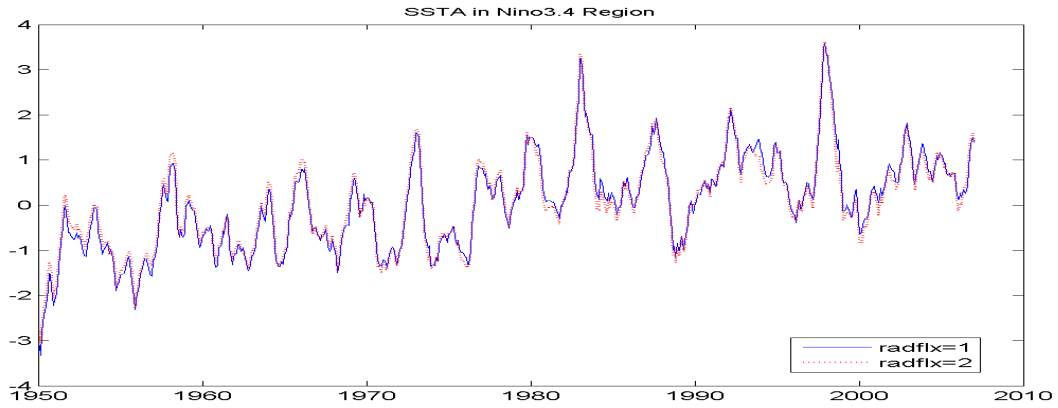
Fig. 7: The HYCOM simulated SST anomalies in Nino3.4 region from 1950 to 2006 a) using the classic bulk formula method, b) using Kara (2000) calculating method.
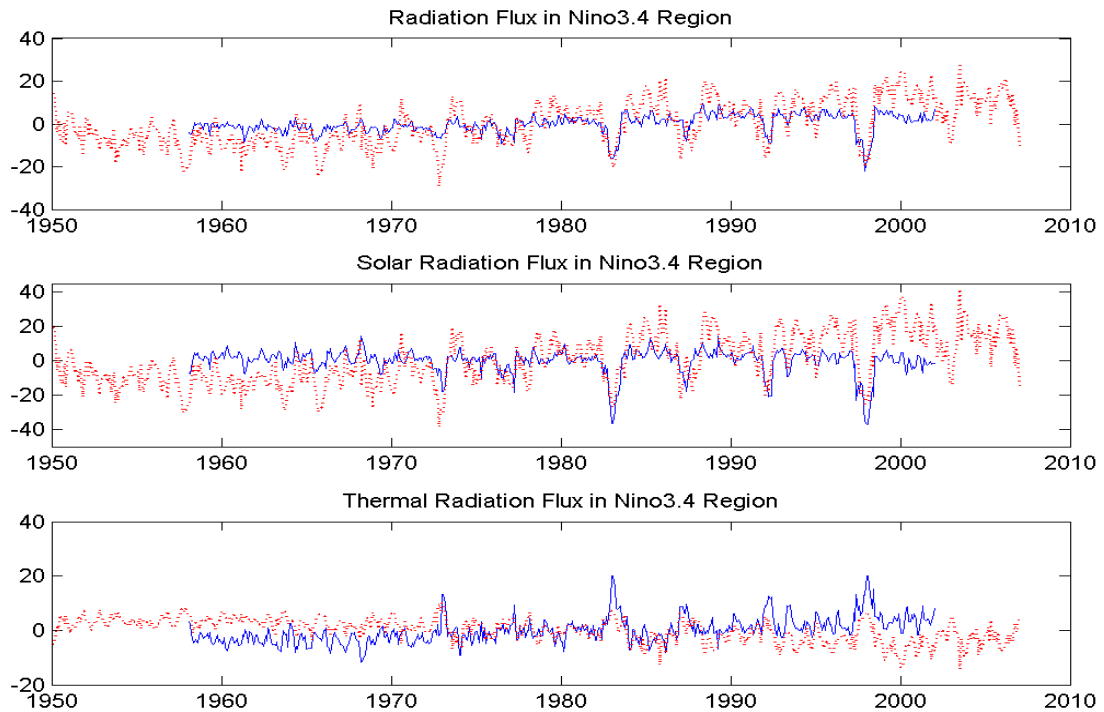
Fig. 8: The a) radiation heat flux anomaly, b) solar radiation flux anomaly and c) thermal radiation flux anomaly in Nino3.4 region from 1950 to 2006 from NCEP (red) and ECMWF (blue) dataset.